

Technische Universität München
Fakultät für Physik



Abschlussarbeit im Bachelorstudiengang Physik

High-precision phase stabilization between microwave generators

Hochpräzise Phasenstabilisierung zwischen Mikrowellengeneratoren

Johanna Fischer

18. Juni 2014

Erstgutachter (Themensteller): Prof. Dr. rer. nat. habil. R. Gross
Zweitgutachter: Prof. Dr. R. Kienberger

Contents

1 Introduction	1
2 Fundamentals	3
2.1 PID-controlling	3
2.2 Temperature sensors	6
2.3 Phase fluctuations	7
3 Experimental Techniques	9
4 Results and discussion	13
4.1 Temperature stabilization	13
4.2 Phase stabilization	25
5 Conclusion and outlook	35
Bibliography	37

Chapter 1

Introduction

Quantum teleportation is a magnificent achievement of modern quantum theory. It exploits non-local correlations between separated quantum systems and allows to implement a disembodied transport of quantum states between two spatially distinct locations. Quantum teleportation can be used in the field of secure communication and for quantum information processing schemes[1] [2].

In the Superconducting Quantum Circuits group of the Walther-Meißner-Institute, we are developing a quantum teleportation experiment with continuous variables. In this context, squeezed vacuum states generated by Josephson parametric amplifiers (JPA) are an essential resource [3]. In particular, these squeezed states are characterized by a squeezing angle which is an important quantity for the quantum teleportation protocol. Details on the physics of squeezed photonic states can be found elsewhere [4].

The quantum teleportation protocol with continuous variables relies on mixing of two squeezed vacuum states with orthogonal squeezing angles. This orthogonality is provided by a precise control of phases of microwave pump tones applied to the JPA. For successful quantum teleportation experiments one has to suppress phase fluctuations of these sources in time. Apart from other influences the important relative phase stability depends on the temperature stability of the microwave generators.

A modified camping cool-box is used to implement the temperature stabilization. We employ additional fans installed in the walls of our box in order to regulate the air flow and, thus, control the temperature of the microwave sources. Temperature sensors on top of the microwave generators are used as input signals for a PID controller. If the actual temperature differs from a certain desired setpoint, this device calculates a feedback signal which sets a rotation speed for the fans. P , I and D stand for the proportional, the integral and the differential parameter, respectively. They determine the amplitude of the feedback signal based on different time scales - P refers to the instantaneous error, I to an integral of the past errors and D to a first derivative of the error. The microwave generators are connected to a network analyzer which measures the phase and the amplitude of each source separately. Thus we can estimate the relative phase difference between the microwave sources and track it versus temperature or time.

For the quantum teleportation experiment we require a microwave tone at a frequency of approximately 12 GHz. Therefore we make a reference measurement with the frequency of 6 GHz which can be later converted to 12 GHz using the "doubler" option in our SGS100 microwave generators. For this frequency it is possible to suppress peak-to-peak fluctuations of the relative phase to 0.5° per hour. According to our preliminary estimations, this phase stability should be sufficient for basic needs of the quantum teleportation protocol.

This work is structured as follows. In Chapter **2** we give a brief overview on the theoretical background of phase fluctuations and PID control (required for real-time temperature stabilization of our system). Chapter **3** introduces the setup we use and how it is constructed. In Chapter **4** we discuss our experimental results and conclusions.

Chapter 2

Fundamentals

2.1 PID-controlling

In this work a PID controller is used to stabilize the temperature in a camping cool-box. In general, PID-controlling is a method that can be used for every process that has a measurable output variable, a desired value for this variable and a method to influence it.

In our case we measure the actual temperature in the box with a temperature sensor and control air circulation through the box. A microwave generator inside of the box provides a heat-load and presents a device-under-test (DUT) system. Air, circulating through the box, is used to cool the DUT. The air circulation is enhanced by fans installed in opposite walls of the box. They both rotate in the same direction. This results in an airflow through the box. In order to stabilize the the temperature of the DUT, the electrical current that causes the rotation of the fans has to react on the changes of the system. Therefore a PID controller from Arroyo Instruments (530-1017 E-585 Series TECPak) provides a feedback signal based on the three parameters P , I and D according to the formula (2.1).

$$I_{\text{feedback}} = P \cdot \varepsilon + I \cdot \int_{t_0}^t \varepsilon dt + D \frac{d\varepsilon}{dt} \quad (2.1)$$

The variable ε stands for the difference between the desired and the actual temperature.

$$\varepsilon(t) = T_{\text{actual}}(t) - T_{\text{setpoint}} \quad (2.2)$$

These three PID parameters have certain physical meanings: P is the proportional parameter. It controls the amplitude of the response directly proportional to the error ε . The P element is also called the response to the present error ε , because the reaction does not depend on previous changes of ε .

The integral parameter I takes into account what has happened to the system from a certain time constant up to the present time. It can be interpreted as an accumulation of the past error. In some cases, it appears that a controller which is only reacting proportional to the error ε needs a long time to reach the actual setpoint. This happens because of overregulating due to a system inertia. This behaviour is shown in Fig. 2.1 for constant $I = 1$ and $D = 1$ and varied P from $P = 0.5$ to $P = 1$ and $P = 2$. Therefore the integral component is important, because it also takes into account the duration of the error that should have been corrected before. This results in an acceleration to the setpoint as it can be seen in Fig. 2.2.

The derivative component corrects for future temperature deviation as it is proportional to the first derivative in time of ε . In a way, the D component estimates an instantaneous slope of the error dependence on time $\varepsilon(t)$ and compensates for it. The corresponding system dynamics for different D parameters can be seen in Fig. 2.3.

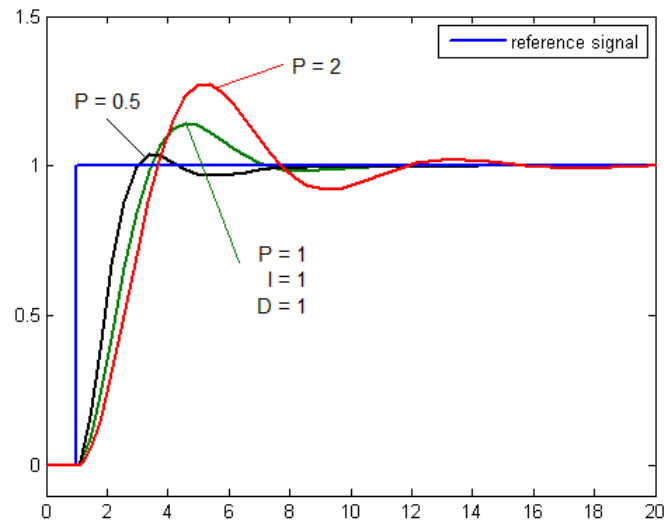


Figure 2.1: The reference signal shows the setpoint change in time $T_{\text{setpoint}}(t)$. The lines of different colors illustrate the corresponding system dynamics for different P values while I and D are constant. As one can see, an excessive P parameter leads to a system instability [5].

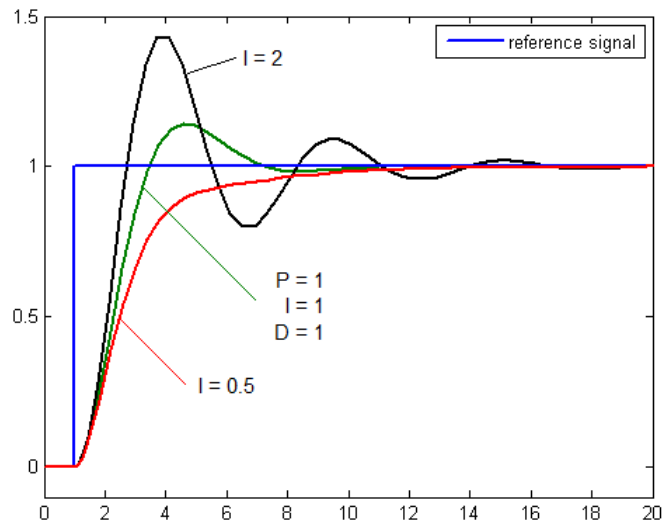


Figure 2.2: The reference signal shows the setpoint change in time $T_{\text{setpoint}}(t)$. The lines of different colors illustrate the corresponding system dynamics for different I values while P and D are constant. The integral parameter accelerates convergence to T_{setpoint} , but extreme I values can cause a temperature overshoot[5].

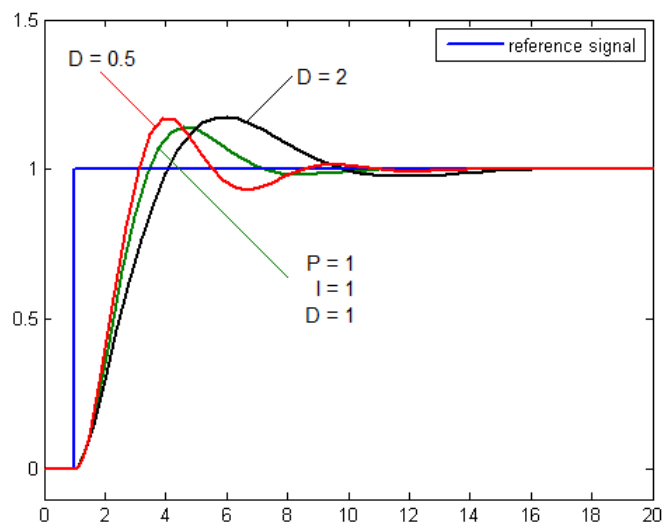


Figure 2.3: The reference signal shows the setpoint change in time $T_{\text{setpoint}}(t)$. The lines of different colors illustrate the corresponding system dynamics for different D values while P and I are constant. The derivative component D helps to dampen oscillatory behaviour while approaching to T_{setpoint} [5].

2.2 Temperature sensors

To stabilize the temperature of the DUT, it is important to measure its exact temperature. For this task we use thin-film platinum sensors [another name - Resistance Temperature Detector (RTD) sensors], whose electrical resistance strongly depends on the ambient temperature. We employ two different kinds of these sensors: a temperature sensor PT100 and a sensor PT10000.

The RTD temperature sensor resistance increases as the temperature increases. RTD sensors can be used in a broad temperature range, as it is shown in Fig. 2.4, from 0 °C to 100 °C. Formula (2.3) describes the resistance dependence R of PT sensors on the temperature T .

The difference between the PT100 and the PT1000 is their resistance R_0 at 0 °C, which corresponds to $R_0 = 100 \Omega$ and $R_0 = 10\,000 \Omega$. Sensors with higher base resistance R_0 produce a higher voltage change over the same temperature range in comparison with less resistive sensors in a situation with a fixed bias current. They may be used in order to improve the temperature resolution when we are limited by an internal resolution of ADC (analog-to-digital) converter.

A and B are material constants: $A = 3.9848 \cdot 10^{-3}$, $B = -0.58700 \cdot 10^{-6}$.

$$R = R_0(1 + AT + BT^2) \quad (2.3)$$

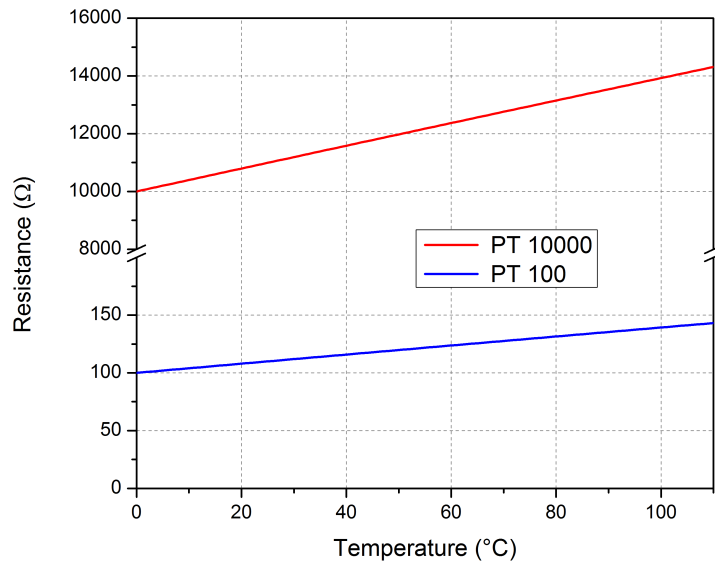


Figure 2.4: Typical temperature dependence of the resistance for the RTD sensors PT100 and PT10000.

2.3 Phase fluctuations

In general, phase fluctuations can be observed in an output signal of every real microwave generator. If an ideal wave function of a sine-signal is:

$$V_{\text{ideal}}(t) = A_0 \cdot \sin(w_0(t)). \quad (2.4)$$

The real signal has a random amplitude and phase:

$$V_{\text{real}}(t) = (A_0 + E(t)) \cdot \sin(w_0(t) + \xi(t)). \quad (2.5)$$

The amplitude noise is $E(t)$ and the phase fluctuations are given by $\xi(t)$.

We assume that we can decrease the relative phase fluctuations between the two RF-sources in our experiment by stabilizing the temperature of the latter. In a typical microwave generator (see Fig. 2.5) a low-frequency signal (typically 10 MHz) from an internal device clock is sent to a synthesizer which generates the high-frequency output. The latter is fed to a pre-amplifier section. Due to technical reasons, it is easier first of all to amplify the synthesizer signal to the maximum possible value and then, attenuate it to the power requested by the user. As the consequence, an additional tunable attenuator is needed. In the synthesizer section a temperature stabilization is integrated. The cooling box with its PID controlled temperature stabilization is used to additionally stabilize the temperature of the output section with the tunable attenuator.

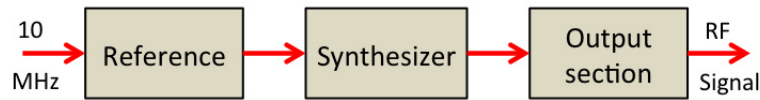


Figure 2.5: General scheme of a microwave generator. A stable low-frequency clock signal is converted to a high-frequency RF signal. Then, it is then amplified in the output section. Finally, a tunable attenuator is used to produce the output signal at the specified amplitude and frequency. For a more detailed information on the particular microwave generator from Agilent Technologies see [6].

We employ a vector network analyzer ZVA24 (from Rohde & Schwarz) to measure phase and amplitude of the high-frequency outputs of the SGS sources. The network analyzer calculates the complex scattering parameter S_{12} for a two-port network [7]:

$$S_{12} = \frac{V_{\text{out}}}{V_{\text{in}}}, \quad (2.6)$$

where V_{in} stands for the detected voltage of the input wave and V_{out} is the voltage amplitude of the output wave. The absolute value of the S-parameter is the amplitude and its argument represents the phase of the analyzed microwave signal.

In our experiment we use the network analyzer to measure the amplitude and the phase of an external microwave signal via measurement of the scattering parameter S_{12} . In this situation, the network analyzer output signal V_{out} provides us with a reference frame for both phase and amplitude, though, effectively, we measure no reflected or transmitted signals but only the signals generated by the external SGS sources. The relative phase ϕ is defined as a simple difference of phases $\phi = \xi_1 - \xi_2$ of two SGS generators. By analyzing the temperature dependence of relative phase we can stabilize it with the PID controlled cooling box.

To compare the measured data it is helpful to calculate the standard deviation σ and the peak-to-peak amplitude A for each measurement. If we measure values x_i that appear N times with the probability P_i , the standard deviation σ_x is defined as it follows:

$$\sigma_x = \sqrt{\frac{1}{N} \sum_{i=1}^N (x_i - \mu)^2}, \text{ where } \mu = \frac{1}{N} \sum_{i=1}^N x_i. \quad (2.7)$$

The peak-to-peak amplitude A is defined as the difference between the maximum and the minimum of the measured variable x in the certain range:

$$A_x = x_{\text{max}} - x_{\text{min}}. \quad (2.8)$$

Chapter 3

Experimental Techniques

In this chapter we describe an experimental set-up for temperature stabilization and phase measurements. To create a temperature stabilized environment for the microwave sources, we put them into a modified camping cool box. The box which is shown in Fig. 3.1 provides thermal isolation from outside and has four separate custom-made chambers. For temperature stabilization we apply PID controlled computer fans. The control signal for the TEC Pak PID controller (shown in figure Fig. 3.2) comes from a temperature sensor which is placed on top of a microwave generator (Fig. 3.3). We use two different sensors of the same type (platinum) but with different base resistance values: the PT100 and the PT1000.

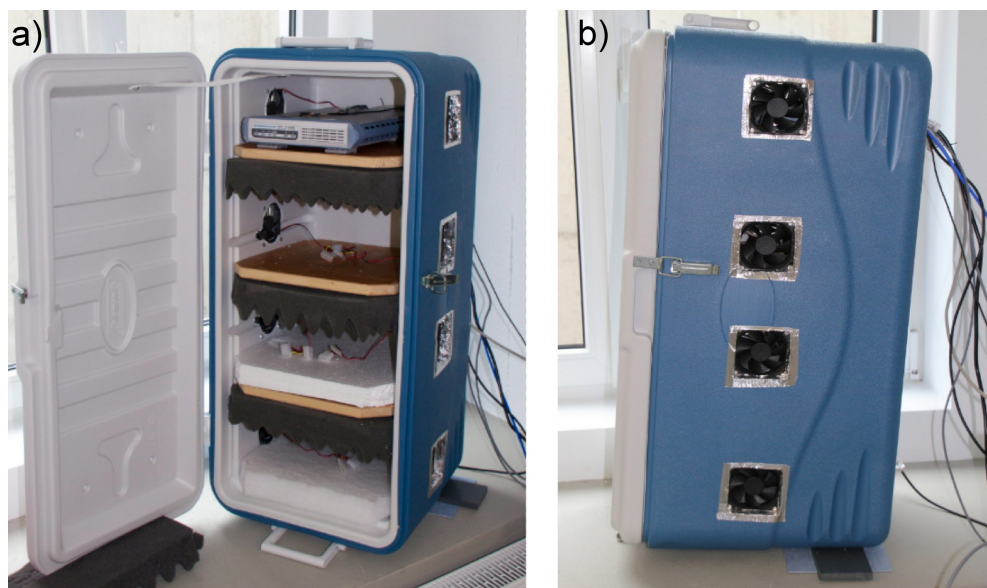


Figure 3.1: Cool box with with PID-controlled fans for the temperature stabilization of the SGS sources. **a)** Opened box with its four separated chambers and one microwave generator inside. **b)** Closed box. Holes for the cables can be found on the backside.



Figure 3.2: TECPak PID controller from Arroyo Instruments. **a)** Front panel with the power cable and the USB connector to the computer. **b)** Front panel with power, USB, RS-232 and analog ports. **c)** Rear panel with one port for the input signal coming from the temperature sensor and the output line for the fans [9].

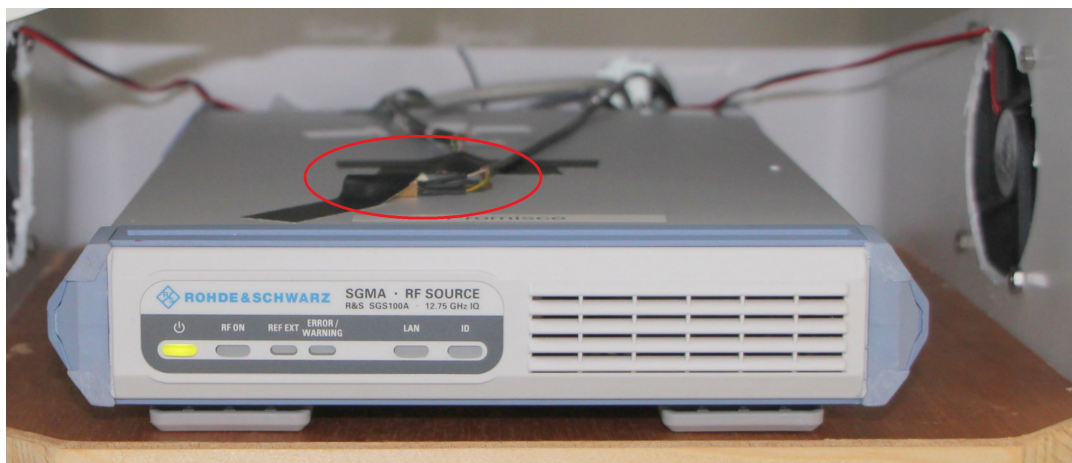


Figure 3.3: Temperature sensor (marked by the red ellipse) on top of the SGS source in the cool box.

First, we test the temperature stability of a single microwave source inside of the isolation box. We look for optimal PID parameters which correspond to smallest temperature deviations of DUT in time. As the second step, we place two microwave generators in one of the four equally designed chambers as we have only one PID TECPak controller available. In future, it is possible to use separate chambers with one PID controller per chamber for separate devices in order to stabilize them independently. For the phase measurements, we employ a vector network analyzer ZVA24 (from Rhode & Schwarz) to measure phases and amplitudes of high-frequency outputs of the microwave sources. We track and analyze the relative phase in time.

The SGS sources are capable of generating RF-signals in the frequency range from 1 MHz to 12.75 GHz. Typically, when using several microwave sources together, one has to synchronize their respective phases. This can be achieved by a phase-locking of their internal clocks to each other [7] with 10 MHz reference signals. In this scenario, one device usually provides a master 10 MHz signal, while the others are phase-locked to the master (see Fig.3.4 **a**). Additionally, a so-called "daisy chain" option is implemented for a better phase-locking of the outputs of several SGS sources, when the frequencies of the output RF-signals of all generators are exactly at the same frequency (Fig.3.4 **b**). In this situation, the high frequency signal from the master source which can be between 80 MHz and 6.5 GHz is directly fed to the slave source via the reference channel. Basically, this slave generator works as a tunable amplifier. This scheme provides a superior control of relative phases in comparison to the usual scheme with the 10 MHz reference. In our experiment, we test both approaches: The 10 MHz reference option (Fig.3.4 **a**) and the "daisy chain" option. There we can, additionally to the 6 GHz output frequency, use a so-called "doubler" option in the SGS microwave sources which allows us to double the frequency from the coherent input to 12 GHz (Fig.3.4 **b**).

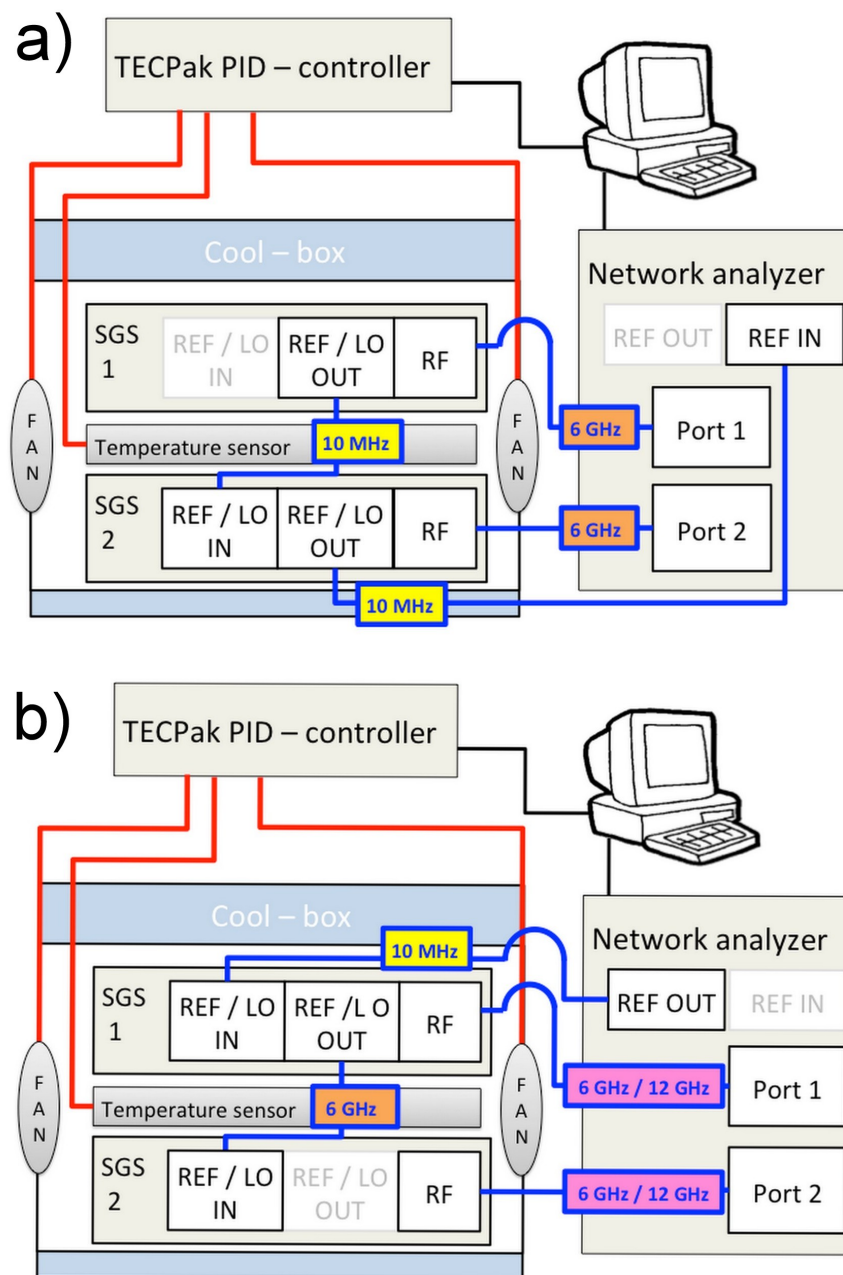


Figure 3.4: Different settings in the experimental setup for the phase measurements. **a)** 10 MHz reference option, 6 GHz output frequency. **b)** "daisy chain" option for 6 GHz and 12 GHz output frequency when the "doubler" option is used.

Chapter 4

Results and discussion

4.1 Temperature stabilization

Here we present results on a temperature stabilization of a single microwave SGS source inside an isolation box for two different temperature sensors PT100 and PT10000.

These sensors are used to provide a control signal to the TEC Pak PID controller. It turns out that for the different sensors, different PID parameters are required to optimize the PID controlled temperature stabilization.

Independently of the sensor, it is important that a temperature setpoint is at least 10 K above the room temperature. The reason for this is that the cooling of the system is caused by an air exchange.

4.1.1 PID parameters for the temperature sensor PT100

In this section we test different PID parameters for the TEC Pak controller from Arroyo Instruments when it is used together with the temperature sensor PT100. It appears, that the three parameters do not exactly behave as they were introduced in Chapter 2. Therefore we have to find out how our system reacts on changes of the PID parameters.

The first step on our quest for optimal PID parameters is to set the proportional parameter to $P = 1$ and the integral parameter to $I = 0.5$, and then test three different values of the differential parameter $D = 30$, $D = 50$ and $D = 100$. There we use a rather large range for the D parameter. As it appears in our system, large D parameters are useful to decrease the amplitude of oscillations around the temperature setpoint T_{setpoint} . This is shown in Fig. 4.1, where the three curves are plotted with the artificial temperature offset of 0.3°C . The setpoint is the same for all these curves ($T_{\text{setpoint}} = 30^\circ\text{C}$). The offset value is introduced artificially during post-processing and serves only for better comparison of the experimental data.

We calculate the standard deviation and the peak-to-peak amplitude for the discussed measurements (see Tab. 4.1). Increasing the D parameter from $D = 30$ to $D = 50$ is helpful to minimize the peak-to-peak-amplitude of the oscillations up to

a value of $A_T = 0.14^\circ\text{C}$ in the black dashed area. But after 10 minutes the temperature oscillates again with $A_T = 0.21^\circ\text{C}$ in the red dashed area. Increasing the D parameter further is not useful, as the amplitude of the oscillations is constantly at 0.23°C for $D = 100$. $D = 50$ also produces the lowest standard deviation ($\sigma_T = 0.038^\circ\text{C}$). This shows us that the differential parameter D can help to dampen oscillatory behaviour while approaching the setpoint temperature, but also that too large D values produce overshoots.

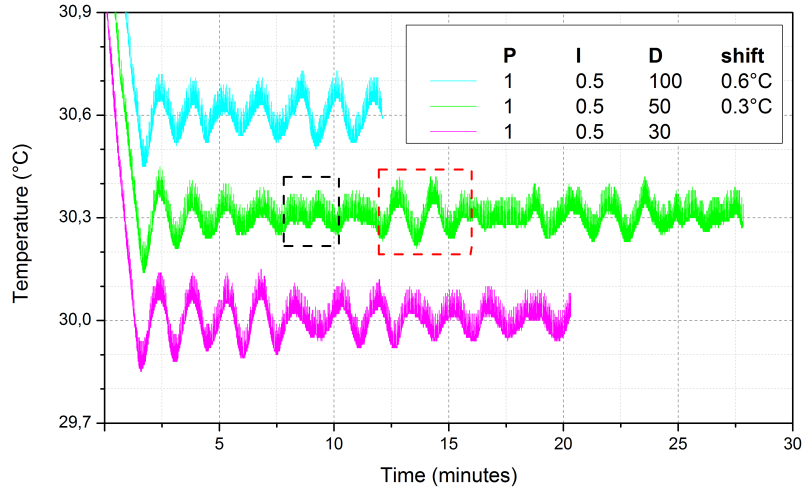


Figure 4.1: Measurements of the temperature stabilized SGS microwave source for certain PID parameters with the temperature sensor PT100. The black dashed box shows the area with better temperature stabilization whereas the peak-to-peak amplitude increases again in the red dashed area. The P and the I parameter are set to constant values in order to optimize the D parameter.

P	I	D	σ_T ($^\circ\text{C}$)	A_T ($^\circ\text{C}$)
1	0.5	100	0.049	0.23
1	0.5	50	0.038	0.21
1	0.5	30	0.048	0.26

Table 4.1: Standard deviations and the peak-to-peak amplitudes for the measurements shown in Fig. 4.1

Our result approximately fits the optimal PID parameters provided by the producer company (Arroyo Instruments) for this temperature sensor ($P = 0.15$, $I = 0.001$, $D = 25$ [8]).

It is remarkable that higher D parameters can be used to reach the setpoint faster. This is shown in Fig. 4.2 for $P = 1$, $I = 0.1$ and $D = 25$ or $D = 50$. The black arrows show the point of convergence for each curve. The artificial temperature offset for the second curve is 1°C .

As we are interested in long periods of time, a fast reach of the setpoint is not as important, as a low amplitude in the oscillation.

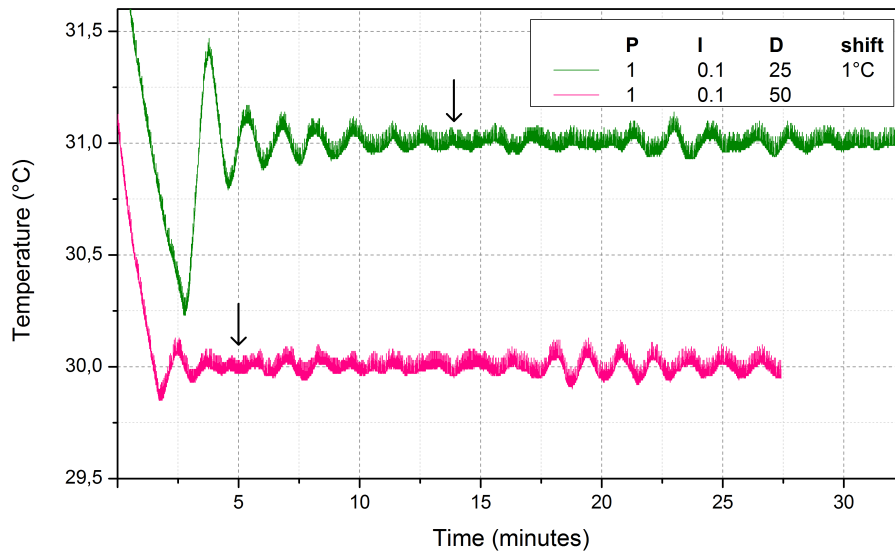


Figure 4.2: Different kinds of convergence to the setpoint temperature for constant P and I values, and for different D values with the temperature sensor PT100. The black arrows show the points of convergence in time.

As a next step we want to optimize the integral parameter I . Therefore we keep $P = 1$ and $D = 50$ constant while changing I . For the integral parameter we try four values from $I = 0$ to $I = 0.5$. The curves are plotted with a temperature offset of 0.3°C . The results are shown in Fig. 4.3. The calculation of the the standard deviations and the peak-to-peak amplitudes for the four graphs can be seen in Tab. 4.2. We observe that small values of the integral parameter like $I = 0.01$ are better than the use of no I parameter, as the standard deviation and the

peak-to-peak amplitude are decreasing. For larger integral parameters like $I = 0.1$ and $I = 0.5$ the standard deviation and the peak-to-peak amplitude grow. Looking at the curve shape we see an increase at the amplitude of temperature oscillations around T_{setpoint} after a certain period of time. We call these areas, highlighted by red dash lines in Fig. 4.3 an "outbreak". It is remarkable that the time until the outbreak seems to decrease with an increasing I parameter. This leads to the assumption that for higher I values the system tends to overshoot faster. As the outbreaks harm the temperature stability, we are not increasing the I parameter further.

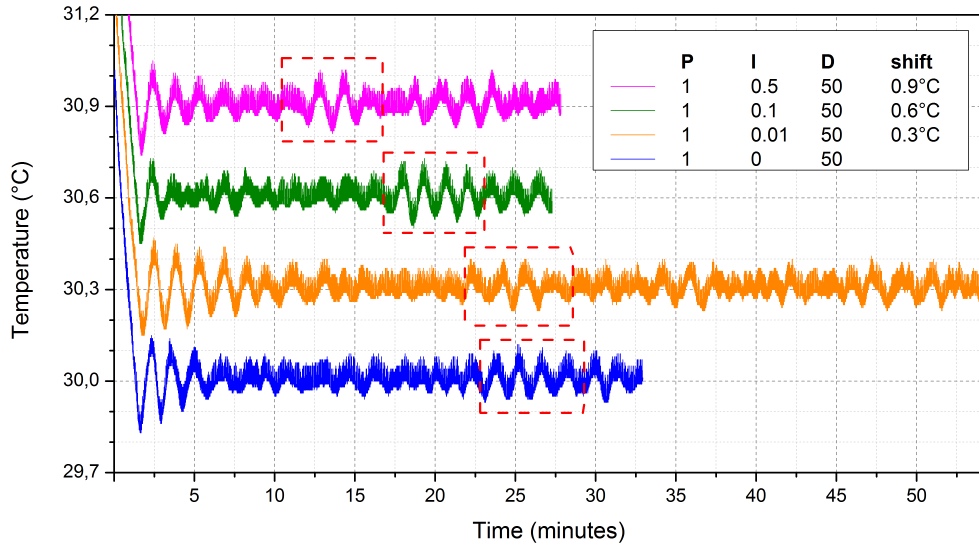


Figure 4.3: Measurements with the PT100 for constant P and D values and various I parameters. The red dashed boxes show the areas of the so-called "outbreaks".

P	I	D	σ_T (°C)	A_T (°C)
1	0.5	50	0.038	0.21
1	0.1	50	0.037	0.23
1	0.01	50	0.034	0.18
1	0	50	0.035	0.19

Table 4.2: Standard deviations and the peak-to-peak amplitudes for the measurements with the PT100 for constant P and D values and various I parameters.

Varying the PID parameters shows, that they do not have an independent behaviour, but their relation to each other is important. In Fig. 4.4 different sets of PID values are shown. We can compare the standard deviations and the peak-to-peak amplitudes in Tab. 4.3. For example increasing P from $P = 0.15$ to $P = 0.8$ and I from $I = 0.05$ to $I = 0.1$ together with an decrease of the D parameter from $D = 30$ to $D = 10$ produces with approximately $\sigma_T = 0.04^\circ\text{C}$ standard deviation and $A_T = 0.2^\circ\text{C}$ peak-to-peak amplitude the same temperature stability.

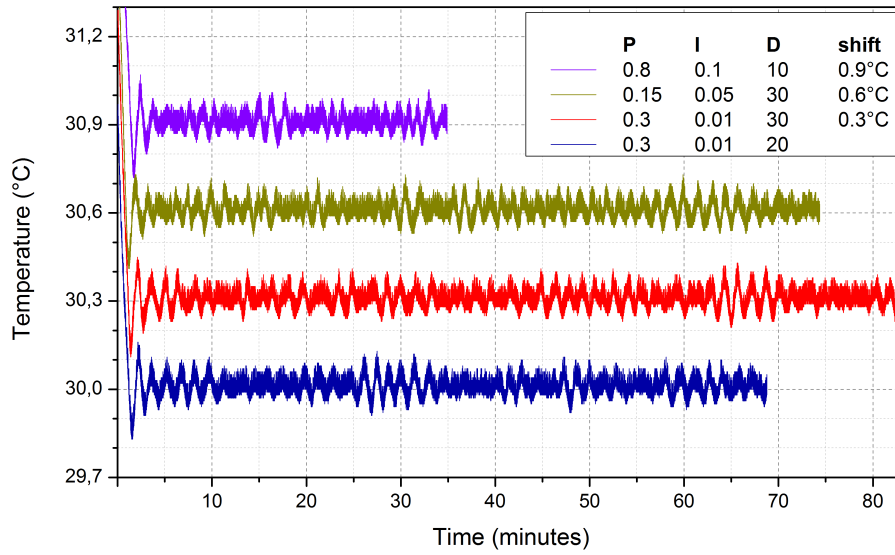


Figure 4.4: Measurement with the PT100 for different PID values to show that parameters in a correct range and relation to each other can compensate the behaviour of each other and produce nearly the same temperature stability.

P	I	D	σ_T ($^\circ\text{C}$)	A_T ($^\circ\text{C}$)
0.8	0.1	10	0.035	0.20
0.15	0.05	30	0.036	0.21
0.3	0.01	30	0.037	0.23
0.3	0.01	20	0.035	0.22

Table 4.3: Standard deviations and the peak-to-peak amplitudes for the measurements with the PT100 for different PID values.

Results for the PID parameters for the temperature stabilization with the PT100 temperature sensor and one SGS source in the cool-box. Summing up our results from the measurements for the PT100 temperature sensor and one SGS source in the cool-box we can state, that it is useful to set the proportional parameter between $P = 0$ and $P = 1$, use integral values smaller than $I = 0.1$ and choose D parameters from $D = 10$ to $D = 30$. In this parameter range we can achieve a temperature stability with $\sigma_T = 0.04^\circ\text{C}$ and $A_T = 0.2^\circ\text{C}$.

For the later following phase measurements (Chapter 4.2) we have to keep in mind, that we have used only one microwave generator in the box, when we were optimizing the PID parameters. It appears that the use of two devices, as we later do to measure the relative phase between them, also influences the behaviour of the PID control. Therefore it always makes sense to test some combination of PID values in the aforementioned range, when the PT100 temperature sensor is used.

4.1.2 PID parameters for the thermistor sensor PT10000

With the temperature sensor PT100 we are able to suppress peak-to-peak fluctuations to $A_T = 0.2^\circ\text{C}$ over a period of 30 minutes. With the optimized PID parameters we are mainly limited by the resolution of the temperature sensor readout circuitry. In the next measurements we employ the RTD sensor PT10000. A higher resistance of this sensor should help us to increase a characteristic voltage drop per 1°C , thus improving the temperature resolution of our controller.

Just as for the PT100, it appears, that the behaviour of the three parameters does not correspond to the ideal one (see Chapter 2). In comparison with the deviations in Chapter 4.1.1, the use of a large integral parameter deteriorates the results while a larger P and a smaller D parameter, such as $P = 10$ and $I = 1$, produce better results. These findings are shown in the following measurements.

We want to start with the I parameter, because even a small integral parameter creates slow oscillations. They have an oscillation period of approximately two minutes and a high deviation from the setpoint, which produces a peak-to-peak value larger than $A_T > 0.5^\circ\text{C}$. This is shown in Fig. 4.5. For the upper curve a temperature offset of 1°C has been added.

In both measurements the targeted setpoint is $T_{\text{setpoint}} = 30^\circ\text{C}$. For the lower curve with $I = 0$ the mean temperature is constantly above this value. A non zero integral parameter can fix this problem as we can see in the upper curve. But as the overall temperature stability gets worse, we set the integral parameter to zero, even though this can be recognized as an additional overall temperature shift of 0.15°C . We can do this, because we are not interested in a certain setpoint, but in a stable temperature in vicinity of 5°C to the setpoint.

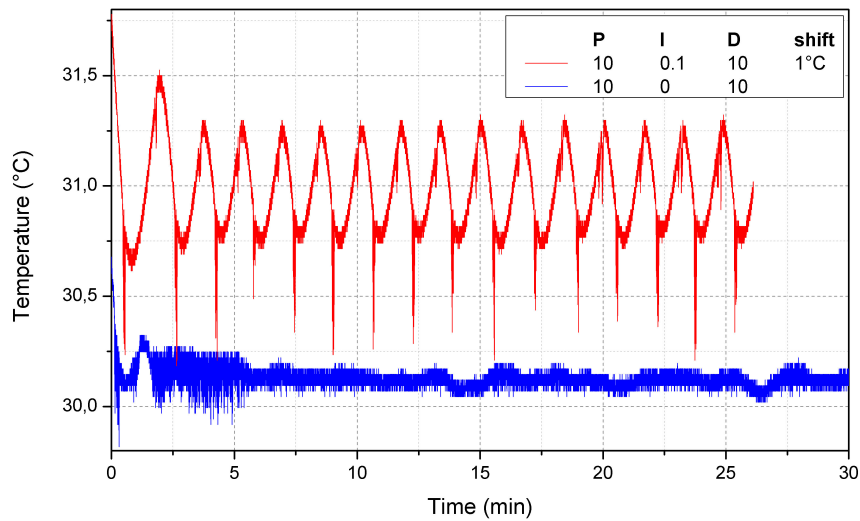


Figure 4.5: Measurement with the temperature sensor PT10000 in order to analyze the influence of the integral parameter.

Additionally, using the new temperature sensor, we have to deal with a new problem. There appear fast temperature drops, that can not be associated with real temperature changes of the microwave generator. A correlation to the current that is sent through the fans can be found. This is illustrated in Fig. 4.6.

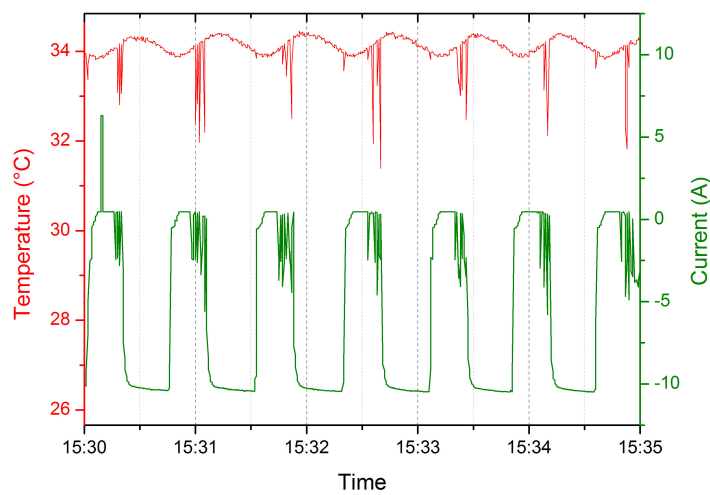


Figure 4.6: Correlation between the temperature and the bias current through the fans for the PT10000. One can notice, that current jumps precede the temperature ones and, probably, artificially create the latter due to a crosstalk between the measurement cables.

For $I = 0$ the other parameters have to be optimized. In Fig. 4.8 and Fig. 4.2 different P values are tested. When D is set to one and $I = 0$, the P parameter has to be larger than $P = 5$ as we can improve the result for $P = 10$. We can suppress the slow oscillations that have a oscillation period of approximately 5 minutes and an amplitude of $A_T = 0.25^\circ\text{C}$ to a flat curve with the fast peak-to-peak oscillations $A_T = 0.15^\circ\text{C}$ (see Fig. 4.2). For this curve we achieve the standard deviation $\sigma_T = 0.028^\circ\text{C}$.

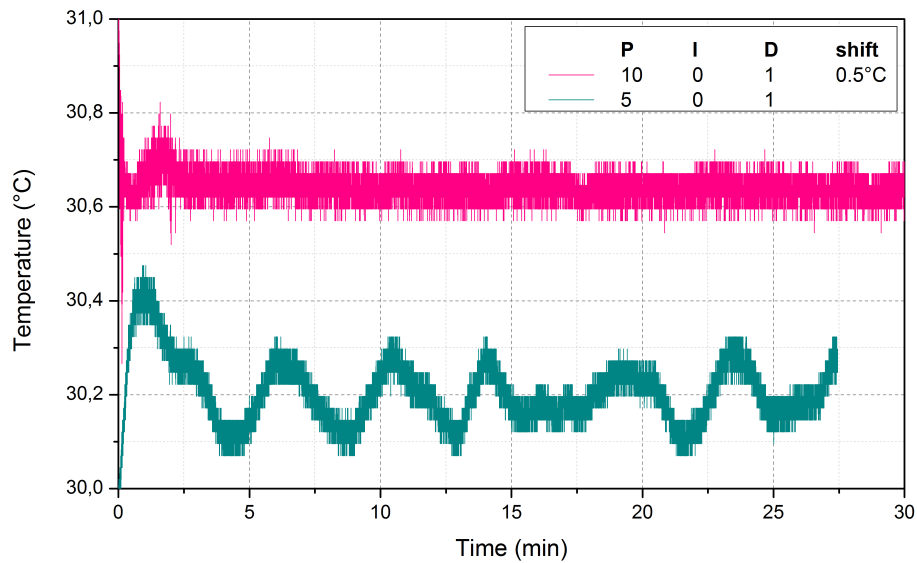


Figure 4.7: Measurement with the PT10000 for two different P values, no integral component and the constant differential parameter $D = 1$. Higher P parameters can be used to suppress slow oscillations with a high amplitude.

In Fig. 4.8 for $D = 10$ we can recognize the aforementioned problem with the fast temperature changes again, when we increase the P parameter over $P = 10$.

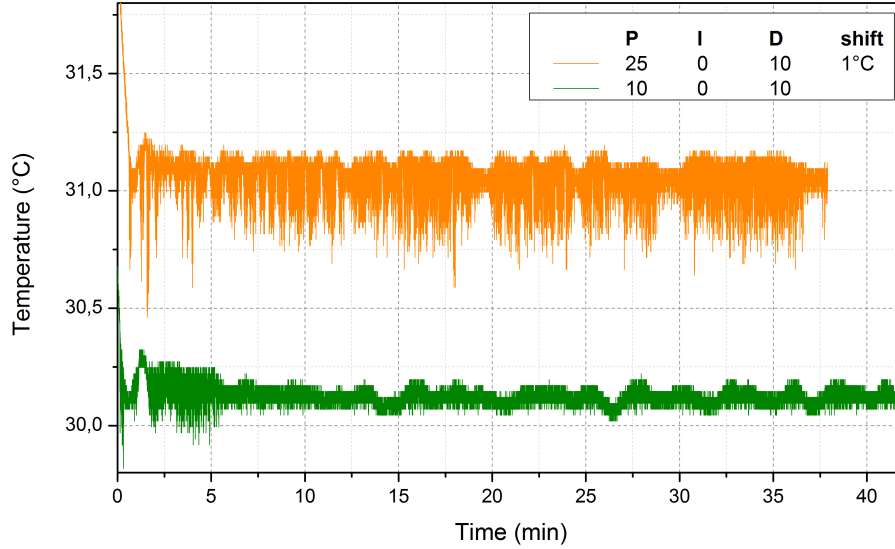


Figure 4.8: Measurement with the PT10000 for two different P values, no integral and a constant differential parameter $D = 1$.

Next we have to find an optimal D parameter for $P = 10$ and $I = 0$: Different D values are plotted in Fig. 4.9. The graphs are again shown with a temperature offset for clarity. The calculation of the standard deviations and the peak-to-peak amplitudes in Tab. 4.4 can not be interpreted clearly at first: For $D = 0.05$ and $D = 0.5$ slow oscillations harmful for the temperature stability can be observed. Between those values for $D = 0.1$ and $D = 1$ the best results are located. The standard deviations for those measurements are approximately $\sigma_T = 0.03^\circ\text{C}$ and the peak-to-peak values equal $A_T = 0.2^\circ\text{C}$. For higher D values the problem with the fast temperature drops appears again. Resuming this measurement we can draw the conclusion that with $P = 10$, $I = 0$ and $D = 0.1$ we achieve the lowest standard deviation and therefore this is the best result we use later on for the phase stabilization.

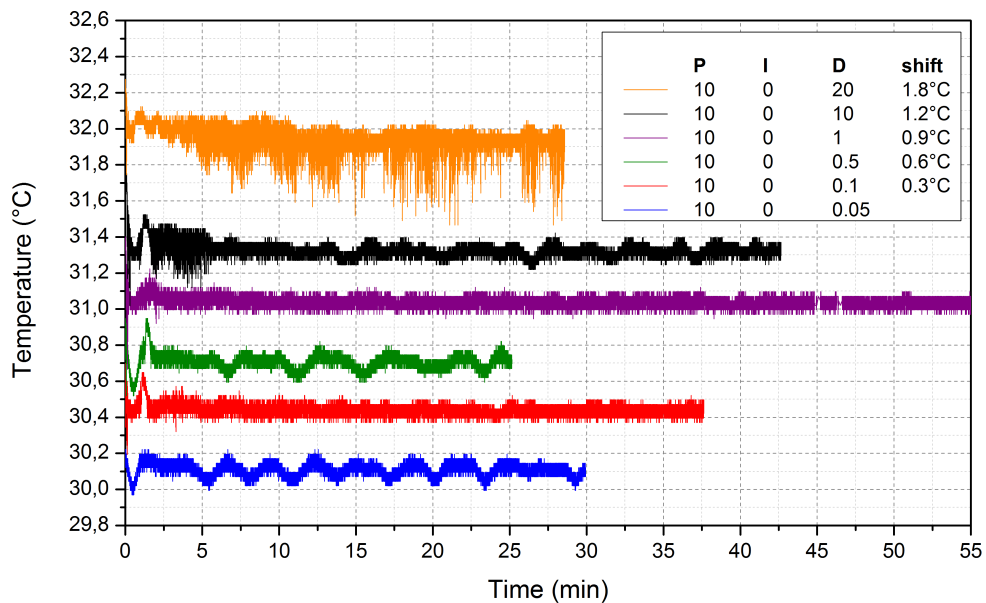


Figure 4.9: Measurement with the PT10000 for $P = 10$, $I = 0$ and various D parameters.

P	I	D	σ_T ($^{\circ}\text{C}$)	A_T ($^{\circ}\text{C}$)
10	0	20	0.072	0.64
10	0	10	0.033	0.33
10	0	1	0.025	0.26
10	0	0.5	0.037	0.23
10	0	0.1	0.029	0.28
10	0	0.05	0.036	0.23

Table 4.4: Standard deviations and the peak-to-peak amplitudes for the measurement with the PT10000 for $P = 10$, $I = 0$ and various D parameters.

PID test over 15 hours. As the next step we test the optimized parameters $P = 10$, $I = 0$, $D = 1$ over a longer period of time. In Fig. 4.10 the results for two measurements with the same parameters are shown with a temperature shift of 0.3°C for the upper curve. Over a period of 15 hours a standard deviation of $\sigma_T = 0.03^\circ\text{C}$ and a peak-to-peak amplitude of $A_T = 0.3^\circ\text{C}$ can be measured. This result is reproducible.

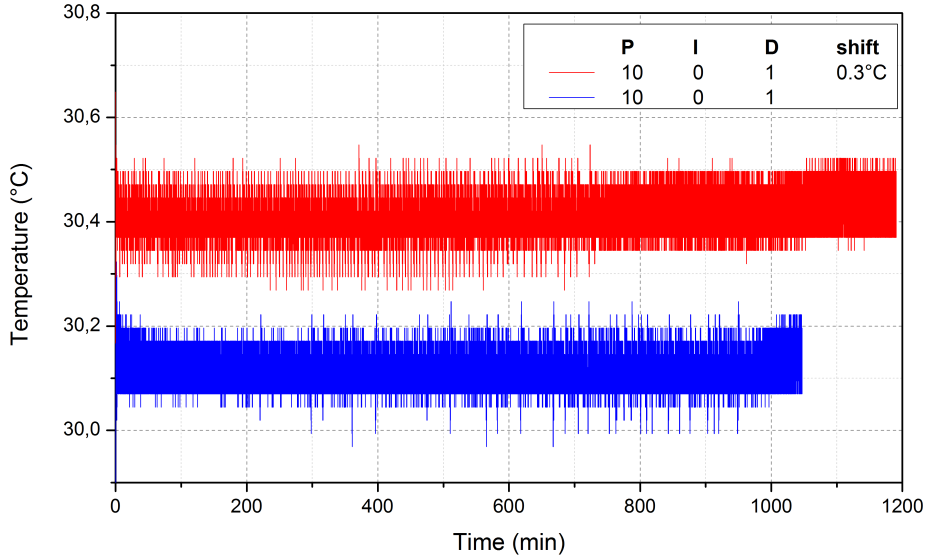


Figure 4.10: Measurement with the PT10000 for a long period of time.

Results for the PID parameters for the temperature stabilization with the PT10000 temperature sensor and one SGS source in the cool-box. Overall, our measurement result for the sensor PT10000 indicate that the non-zero integral parameter I always produces worse results than $I = 0$. So we set the integral parameter $I = 0$ for all future measurements with PT10000. For the proportional parameter we find out, that small P parameters such as $P = 5$ correspond to slow oscillations with an amplitude of $A_T = 0.2^\circ\text{C}$. Further increase of the proportional component to $P \sim 25$ leads to fast non-physical oscillations of the device temperature. Probably, this happens due to an enhanced cross-talk between the measurement and the feedback channels. Therefore, the value of $P \simeq 10$ is the optimal value.

The calculation of the standard deviations and peak-to-peak amplitudes in Fig. 4.4

shows that our system produces the best temperature stability for $D = 1$ with the standard deviation of $\sigma_T = 0.025^\circ\text{C}$ and the peak-to-peak amplitude of $A_T = 0.26^\circ\text{C}$.

Therefore we test the configuration $P = 10$, $I = 0$ and $D = 1$ for more than 15 hours and achieve reproducibly a standard deviation of $\sigma_T = 0.03^\circ\text{C}$ and a peak-to-peak amplitude of $A_T = 0.3^\circ\text{C}$.

Comparing the results for the PID parameters for the temperature stabilization with the PT100 and the PT10000 temperature sensor and one SGS source in the cool-box. Our results for the two temperature sensors show that they produce approximately the same temperature stability. But the limiting factors seem to be different. For the sensor PT100 the temperature resolution limits the performance of our set-up, while for the sensor PT10000 there is a problem of fast temperature changes, presumably due to the enhanced cross-talk between the feedback and temperature measurement cables.

4.2 Phase stabilization

Now we can use the developed temperature stabilization scheme in order to investigate its influence on phase stability of microwave generators SGS100 from Rhode & Schwarz. We test it by stabilizing the temperature of two generators at the same time, measuring phases of their respective RF-signals, and calculating a relative phase deviation in time as described in Chapter 3.

The first tests are done with the PT10000 temperature sensor and the PID values $P = 10$, $I = 0$ and $D = 1$. Later, we switch back to the PT100 sensor.

10 MHz reference option, 6 GHz output frequency. Here we use the 10 MHz reference as it is shown in Fig. 4.11. The microwave output signal of both microwave generators is set at the frequency of 6 GHz and the power at -10 dBm.

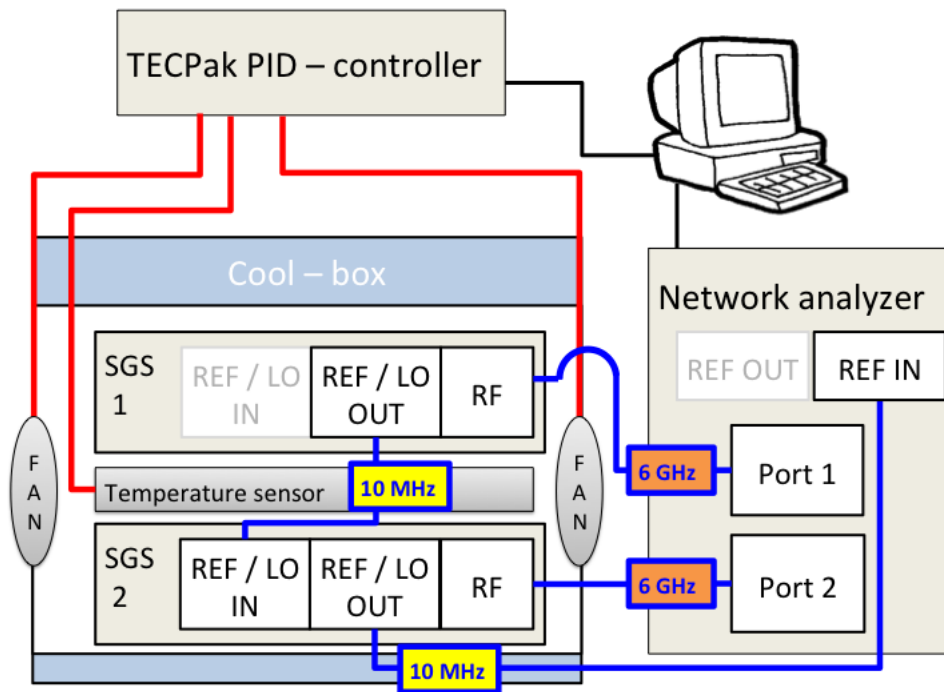


Figure 4.11: Experimental set-up for the phase measurement with the 10 MHz reference option and 6 GHz output frequency.

Fig. 4.12 shows a reference measurement over a full day without the temperature stabilization. We can see that the amplitude of the relative phase deviation is large in this case. The peak-to-peak amplitude is $A_\phi = 40.04^\circ$ and the standard deviation $\sigma_\phi = 8.92^\circ$. The next measurement, illustrated in Fig. 4.13, is done for the same microwave settings, but with the switched ON temperature PID control (using the parameters $P = 10$, $I = 0$ and $D = 1$).

Surprisingly, we observe that the temperature stabilization does not improve the relative phase stability. The peak-to-peak amplitude is $A_\phi = 49.59^\circ$ and the standard deviation $\sigma_\phi = 10.48^\circ$. A possible explanation for this is that we are limited by phase noise of a reference clock in the microwave generators. This clock has an internal temperature control and therefore is not influenced by our additional PID control.

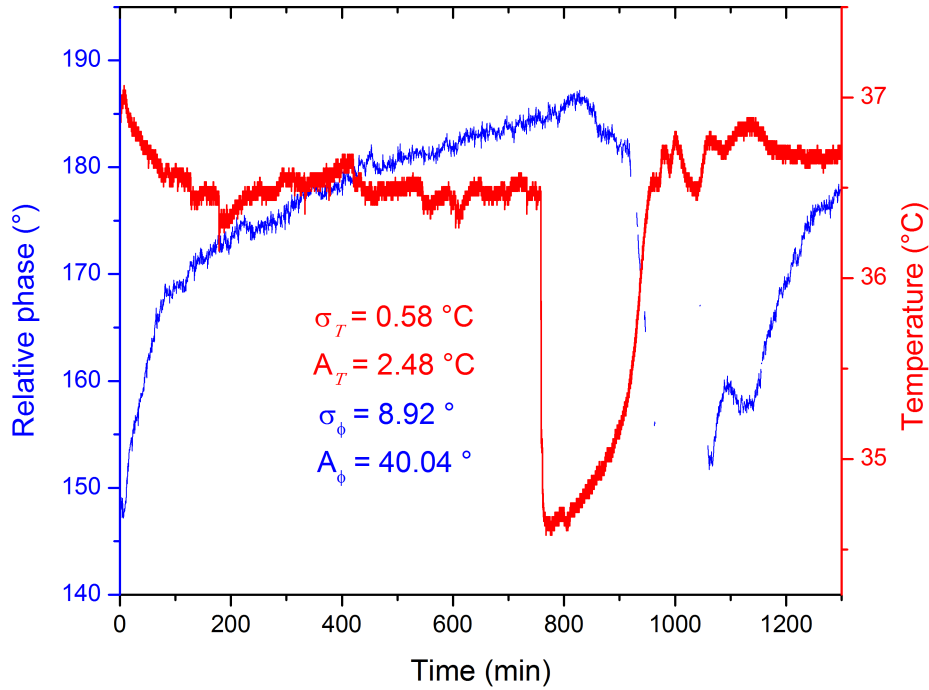


Figure 4.12: Measurement of the temperature with the sensor PT10000 and the relative phase between two SGS sources over a full day. Microwave synchronization is performed via 10 MHz reference signal. Microwave output frequency is at 6 GHz. No temperature control.

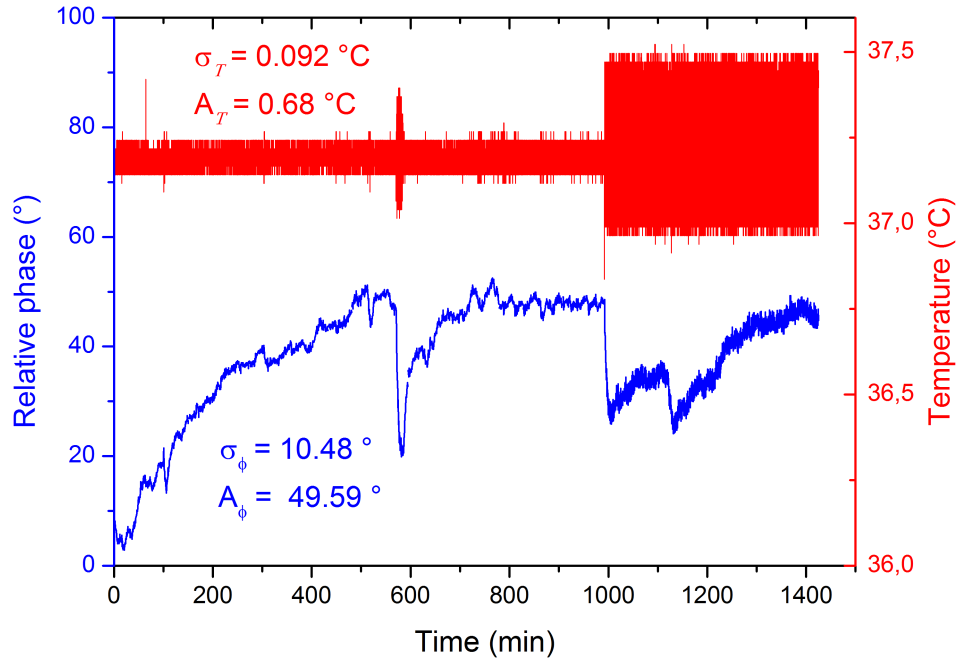


Figure 4.13: Measurement of the temperature with the sensor PT10000 and the relative phase between two SGS sources. Microwave synchronization is performed via 10 MHz reference signal. Microwave output frequencies of the generators are set at 6 GHz. The temperature is stabilized with the PID parameters: $P = 10$, $I = 0$ and $D = 1$.

”daisy chain” option, 6 GHz output frequency. As the 10 MHz reference option shows no improvement together with the temperature stabilization, we now use the local oscillator of one of the SGS sources as a coherent reference input with a frequency of 6 GHz to the other one. This option which is illustrated in Fig. 4.14 is also called ”daisy chain” option.

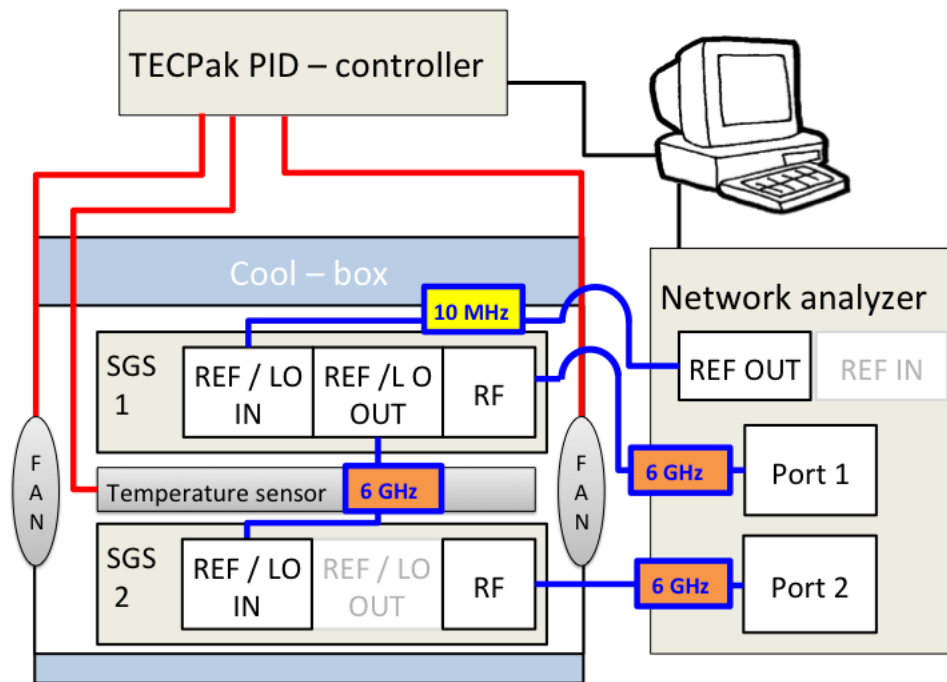


Figure 4.14: Experimental set-up for the phase measurement with the "daisy chain" option at 6 GHz output frequency.

Fig. 4.15 and Fig. 4.16 show the results of phase measurements without and with the temperature stabilization respectively. We can see that with the same PID controlled temperature stabilization it is possible to improve the phase stability from $\sigma_\phi = 0.35^\circ$ to $\sigma_\phi = 0.12^\circ$ and to suppress the peak-to-peak fluctuations A_ϕ from $A_\phi = 1.87^\circ$ to $A_\phi = 0.83^\circ$ per day.

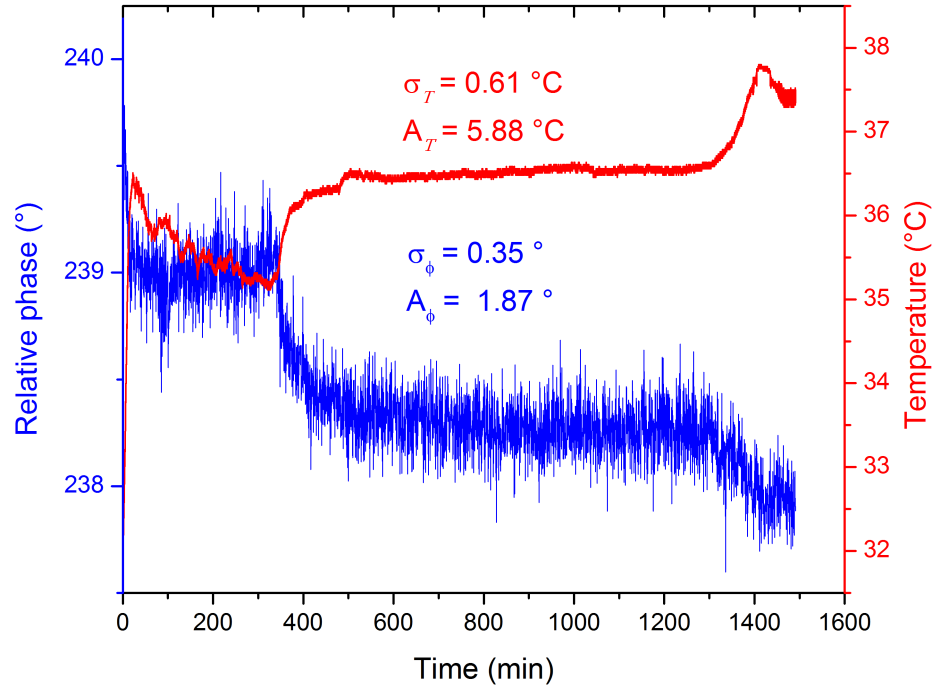


Figure 4.15: Measurement of the temperature with the sensor PT10000 and the relative phase between two SGS sources over one day. Microwave synchronization is performed via "daisy chain" option. Microwave output frequencies of the generators are set to 6 GHz. No PID temperature control is applied. One may notice a strong correlation between the temperature and the relative phase.

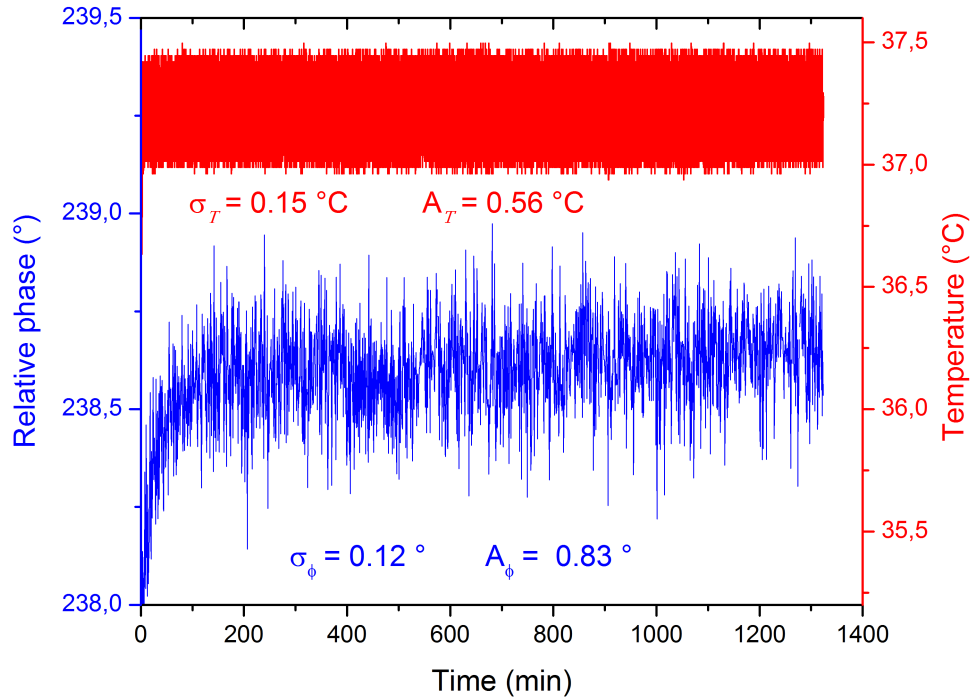


Figure 4.16: Measurement of the temperature with the sensor PT10000 and the relative phase between two SGS sources. Microwave synchronization is performed via the "daisy chain" option. Microwave output frequencies of the generators are set to 6 GHz. The temperature is stabilized with the PID parameters: $P = 10$, $I = 0$ and $D = 1$.

We can compare of the two reference measurements without PID control for the first settings (see Fig. 4.12 and Fig. 4.15). There we can see that without the PID control the phase stability is already better for the "daisy" chain option. But for this option we can suppress phase fluctuations even more when we are stabilising the temperature. That means temperature stabilization makes sense, but it is only useful for the "daisy chain" options.

”Daisy chain” option, 12 GHz output frequency with the use of the ”doubler” option. As mentioned in the beginning of this thesis, we are interested in stabilizing the relative phase of 12 GHz signals. Unfortunately, we cannot straightforward use the ”daisy chain” option for this, as it is limited by the upper frequency of 6.5 GHz. However, there is a so-called ”doubler” option in the SGS microwave source which allows one to double the frequency from the coherent input. It means, that we can use the ”daisy chain” for the 6 GHz signal together with this ”doubler” option in order to generate two coherent signals at 12 GHz phase-locked to each other at 6 GHz bandwidth. The experimental setting for this option is shown in Fig. 4.17.

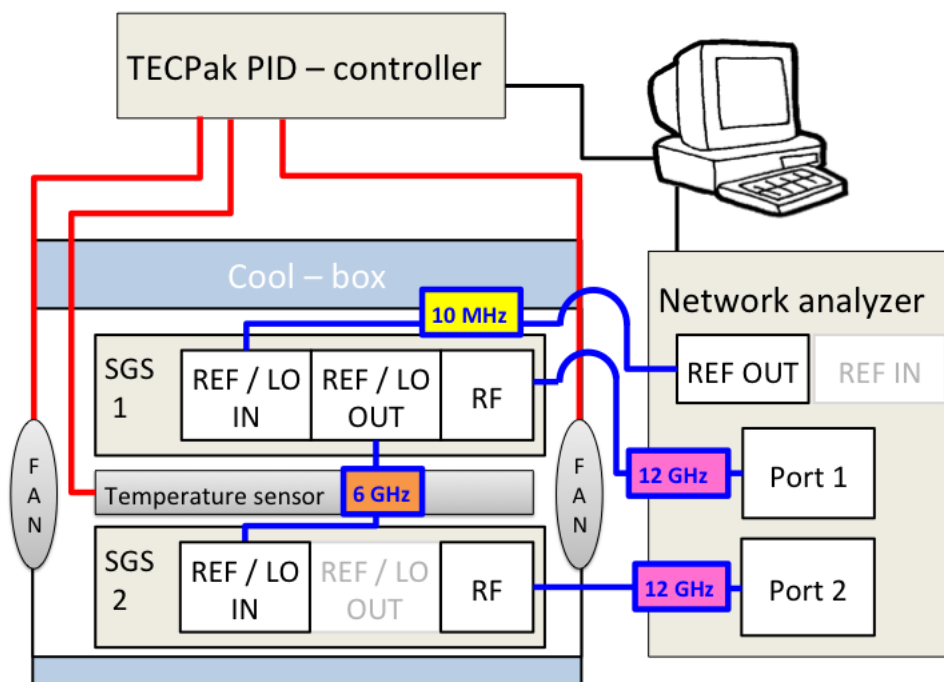


Figure 4.17: Experimental set-up for the phase measurement with the ”daisy chain” option, 12 GHz output frequency and the use of the ”doubler” option.

As the temperature stabilization deteriorates due to the the aforementioned problem with the temperature sensor PT10000 (see Chapter 4.2.1), we try different PID parameters in order to improve the standard deviation of temperature in time σ_T .

Fig. 4.19 shows worse results in the temperature stability, because we try different PID parameters ($P = 5$, $I = 0.1$, $D = 0.5$) but this did not improve the situation. With this we can not reproduce the same stability from the 6 GHz ”daisy chain”

option for the "doubler" option. We receive: $\sigma_T = 0.31^\circ\text{C}$ and $A_T = 3.22^\circ\text{C}$ for the temperature and $\sigma_\phi = 0.42^\circ$ and $A_\phi = 3.19^\circ$ for the phase stability.

Using this measurement as a reference with a bad temperature stabilization, we return to the PT100 sensor now to avoid the problem with the fast temperature drops, even though it has a worse temperature resolution.

Fig. 4.18 shows the measurement for the sensor PT100 with $P = 0.15$, $I = 0.05$, and $D = 30$. The temperature stability is improved to $\sigma_T = 0.22^\circ\text{C}$ and $A_T = 0.79^\circ\text{C}$ and the relative phase stability between two microwave signals at 12 GHz at the level of $\sigma_\phi = 0.26^\circ$ and $A_\phi = 1.96^\circ$.

From those two results we can see clearly that the temperature stability is correlated to the phase stability in our targeted 12 GHz option.

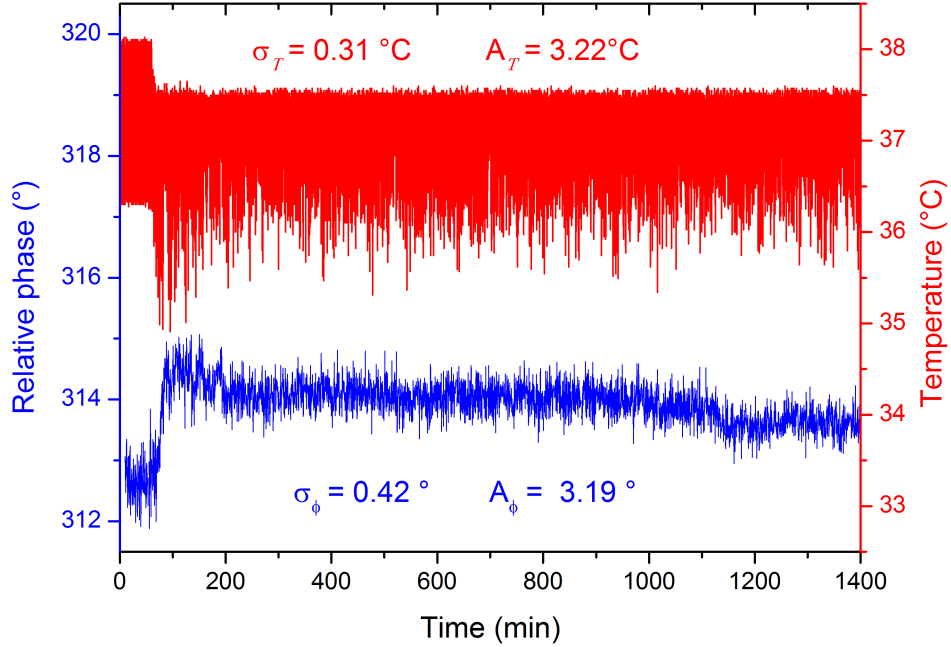


Figure 4.18: Measurement of the temperature with the sensor PT10000 and the relative phase between two SGS sources. Microwave synchronization is performed via the "daisy chain" option. Microwave output frequencies of the generators are set to 12 GHz with the use of the "doubler" option. The temperature is stabilized with the PID parameters: $P = 5$, $I = 0.1$ and $D = 0.5$.

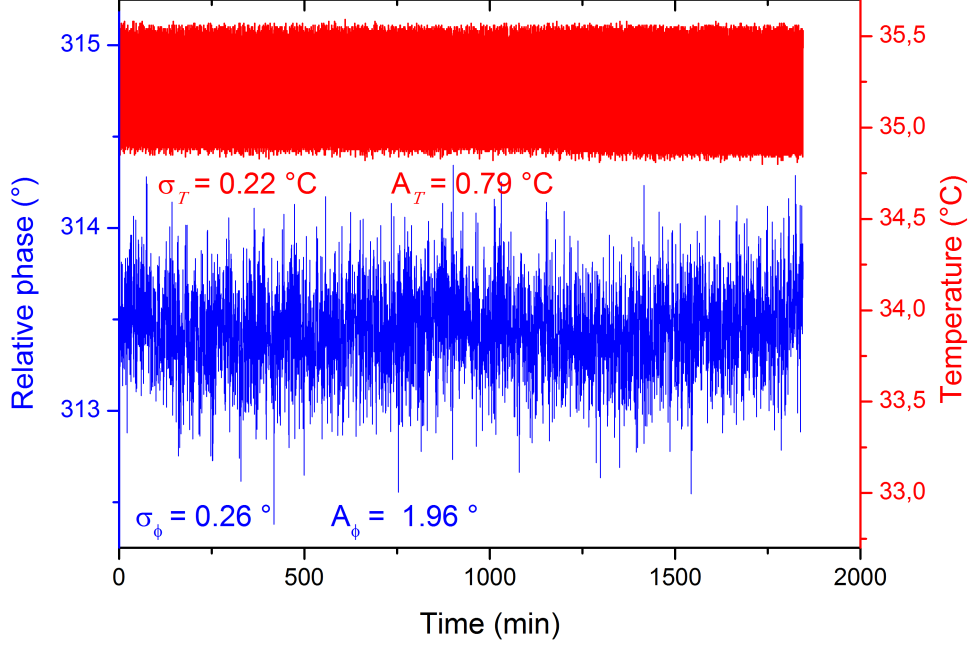


Figure 4.19: Measurement of the temperature with the sensor PT100 and the relative phase between two SGS sources. Microwave synchronization is performed via the "daisy chain" option. Microwave output frequencies of the generators are set to 12 GHz with the use of the "doubler" option. The Temperature is stabilized with the PID parameters: $P = 0.15$, $I = 0.05$ and $D = 30$.

Summing up the results to the different phase measurement options. In Tab. 4.5 the results for the phase stabilization are shown. There are three options presented. For the first one, using a 10 MHz reference signal and a 6 GHz output RF tone, we can not improve the phase stability with a temperature stabilization. For the second one which is a "daisy chain" option at 6 GHz output frequency, we achieve $\sigma_\phi = 0.12^\circ$ and $A_\phi = 0.83^\circ$. For the targeted option with 12 GHz output frequency, we can produce $\sigma_\phi = 0.26^\circ$ and $A_\phi = 1.96^\circ$. Comparing this result to the previous one at the same frequency but a worse temperature stability due to the use of the other sensor and not optimal PID values, we can demonstrate that decreasing σ_T by 0.11°C decreases σ_ϕ by 0.16° .

REF	RF out	PID	Sensor	σ_T ($^{\circ}\text{C}$)	A_T ($^{\circ}\text{C}$)	σ_{ϕ} (deg)	A_{ϕ} (deg)
10 MHz	6 GHz	OFF	PT10000	0.58	2.48	8.92	40.04
10 MHz	6 GHz	ON	PT10000	0.092	0.68	10.48	49.59
"dc"	6 GHz	OFF	PT10000	0.61	5.88	0.35	1.87
"dc"	6 GHz	ON	PT10000	0.15	0.56	0.12	0.83
"dc"	12 GHz	ON	PT10000	0.31	3.22	0.42	3.19
"dc"	12 GHz	ON	PT100	0.22	0.79	0.26	1.96

Table 4.5: Standard deviations and the peak-to-peak amplitudes for the phase measurements, including the values for the temperature. REF stands for the used reference option that can be either the 10 MHz reference signal or the "daisy chain" option "dc". The values marked by green color represent our best results.

Chapter 5

Conclusion and outlook

In this work we use temperature stabilization to achieve a constant relative phase between two microwave sources over the period of one day.

In Chapter 4.1 the two temperature sensors PT100 and PT10000 were employed to stabilize the temperature of a single microwave generator in a special temperature-isolation box. For optimized PID parameters, this is realized with the standard deviation $\sigma_T = 0.04^\circ\text{C}$ and the peak-to-peak amplitude $A_T = 0.2^\circ\text{C}$ for PT100 and a period of one hour.

Using the temperature sensor PT10000 we reproducibly achieve the standard deviation $\sigma_T = 0.03^\circ\text{C}$ and the peak-to-peak amplitude $A_T = 0.3^\circ\text{C}$ for a period of 15 hours with the PID parameters $P = 10$, $I = 0$, $D = 1$.

This PID controlled temperature stabilization is then tested together with measurements of the relative phase between two microwave generators (Chapter 4.2). If those sources are referenced with an external 10 MHz signal, temperature stabilization does not improve the phase stability.

With a "daisy chain" option we achieve the best improvement for an output microwave tone at 6 GHz with $\sigma_\phi = 0.12^\circ$ and $A_\phi = 0.83^\circ$. For this measurement we use the PT10000 temperature sensor with the PID parameters: $P = 10$, $I = 0$ and $D = 1$. The improvement can be seen in comparison to the reference measurement without temperature stabilization where $\sigma_\phi = 0.35^\circ$ and $A_\phi = 1.87^\circ$ per day.

For the targeted frequency of 12 GHz we combine the "daisy chain" with the "doubler" option of the microwave source. Nevertheless, we reach $\sigma_\phi = 0.26^\circ$ and $A_\phi = 1.96^\circ$. We switch to the temperature sensor PT100 for this measurement and achieve a standard deviation $\sigma_T = 0.22^\circ\text{C}$ and peak-to-peak amplitude $A_T = 0.79^\circ\text{C}$ for the 12 GHz option. Thus we can produce a phase stability which is good enough for our future measurements and see clearly the positive influence of temperature stabilization on the relative phase between two microwave output signals at 12 GHz.

Our results show that temperature stabilization has a remarkable influence on the phase stability for the targeted microwave output frequency of 12 GHz, which is needed for the quantum teleportation experiment. For this reason the PID controlled cool box will certainly be useful in future phase-sensitive experiments.

Bibliography

- [1] C. H. Bennet and D. P. DiVincenzo, *Quantum information and computation*, Nature **404**, 247-255 (2000).
- [2] R. Horodecki, P. Horodecki, M. Horodecki and K. Horodecki, *Quantum entanglement*, Rev. Mod. Phys. **81**, 865 (2009).
- [3] L. Zhong, E. P. Menzel, R. Di Candia, P. Eder, M. Ihmig, A. Baust, M. Haerberlein, E. Hoffmann, K. Inomata, T. Yamamoto, Y. Nakamura, E. Solano, F. Deppe, A. Marx and R. Gross, *Squeezing with a flux-driven Josephson parametric amplifier*, New Journal of Physics **15**, 125013 (2013).
- [4] D. F. Walls and G. J. Milburn, *Quantum Optics* (Springer-Verlag, 2008).
- [5] http://en.wikipedia.org/wiki/PID_controller
- [6] *Reducing Phase Noise at RF and Microwave Frequencies*, Agilent Technologies (2011), <http://cp.literature.agilent.com/litweb/pdf/5990-7529EN.pdf>
- [7] D. M. Pozar, *Microwave Engineering* (John Wiley and Sons, 2012).
- [8] Arroyo Instruments, private communication.
- [9] *TECPak 585 user's manual*, Arroyo Instruments (2013), www.arroyoinstruments.com

Acknowledgement

I express my gratitude to all colleagues especially to the members of the Superconducting Quantum Circuits group of the Walther-Meißner-Institute. Despite the risk of giving not explicit credit to everyone who deserves it, I would like to give my special thanks to some people in particular:

Prof. Dr. Rudolf Gross for giving me the opportunity to work in his institute and his interest in my work, even though his time is limited.

Dr. Frank Deppe for the cooperation, for all his ideas and explanations and for proofreading this thesis.

Dr. Kirill Fedorov for his numerous explanations, for his corrections and proofreading of my bachelor thesis and the corresponding presentation. I learned a lot and had a great time, because of his helpful and patient advice in a great atmosphere.

Ling Zhong for her introduction to the daily routine in the laboratory and the help with the measurements and their analysis.

The **technical staff** of the Walther-Meißner-Institute for the advice to build the cooling box.